Received: 29 August 2019 | Revised: 20 November 2019 | Accepted: 25 November 2019

DOI: 10.1002/jhet.3855

WILEY

ARTICLE

Synthesis of novel quinoline-thiosemicarbazide hybrids and evaluation of their biological activities, molecular docking, molecular dynamics, pharmacophore model studies, and ADME-Tox properties

Dhaval B. Patel[1] | **Drashti G. Darji**[1] | **Krupa R. Patel**[1] | **Dhanji P. Rajani**[2] | **Smita D. Rajani**[2] | **Hitesh D. Patel**[1]

[1]Department of Chemistry, School of Sciences, Gujarat University, Ahmedabad, India

[2]Microcare Laboratory and Tuberculosis Research Centre, Surat, India

Correspondence
Hitesh D. Patel, Department of Chemistry, School of Sciences, Gujarat University, Ahmedabad, Gujarat, India.
Email: drhiteshpatel1@gmail.com

Funding information
GUJCOST, Grant/Award Numbers: MRP/2017-18/2323, GUJCOST/MRP/2017-18/2323

Abstract

In the present study, a novel series of *N*-((substituted)carbamothioyl)-2, 4-dimethylquinoline-3-carboxamide (**7a**-**7s**) was synthesized by microwave-assisted method. Structure of these derivatives was examined by spectroscopic techniques such as ^{1}H NMR, ^{13}C NMR, FT-IR, and ESI-MS. Further, the novel synthesized compounds were evaluated for their in-vitro biological activities against antibacterial, antifungal, antimalarial, and antituberculosis activity as well as for in-silico study. The antimalarial results demonstrated that compounds **7c** and **7q** (0.02 μg/mL) have notable potency against *Plasmodium falciparum* compared with chloroquine (0.02 μg/mL); compounds **7l** (0.10 μg/mL), **7e**, **7s** (0.19 μg/mL), **7b**, **7p** (0.15 μg/mL), **7a**, **7f**, and **7f** (0.25 μg/mL) also exhibited good activity against *P. falciparum* compared with quinine (0.26 μg/mL) as standard drug. Docking was performed on *PFDHFR-TS*, given the effect of compounds against the *P. falciparum* strain was excellent in comparison with standard drug. Molecular docking suggested that compounds **7b**, **7i** and **7c**, **7e**, and **7l** closely bind with the active site of protein *3JSU* and *4DP3*, respectively, and compared with biological activity. We have also carried out molecular dynamics simulation on the best dock compound **7e** complex with PDB: *3JSU* to check the stability of docked complex and their molecular interaction. The calculated ADME-Tox descriptors for the synthesized compounds validated good pharmacokinetics properties, suggesting that these compounds could be used as hit for the development of the new active agents.

1 | INTRODUCTION

In the recent decade, quinoline and their derivatives are much familiar in heterocyclic chemistry. These molecules have great importance to biologists and chemists, as they are found in the naturally occurring molecules and also chemically useful moiety having a wide range of biological activity.[1] A quinoline derivatives have been reported to show various biological activities such as antiviral,[2] anticancer,[3,4] antimalarial,[5] antibacterial,[6] antifungal,[7] antituberculosis,[8] antiobesity,[9] anti-inflammatory,[10,11] antibiotic,[12] antihypertensive,[13] tyrokinase PDGF-RTK inhibiting agents,[14] and anti HIV activities.[15,16] In addition to that, substituted quinolines have been employed in the study of metal complex[17] and bio-organometallic process.[17,18] Because of their wide range of applications in the various fields such as industry, medicinal, bioorganic, and synthetic chemistry,

quinoline moiety has become attractive in recent scenarios.

In chemical methods, major effects towards the environment are due to the consumption of energy for heating.[19] To deal with this problem, the development of efficient methods that use another energy source such as microwave irradiation are highly attractive. Nowadays, microwave-assisted synthesis is a new and quickly developing field in organic synthesis.[19] This method is based on critical observation that some reaction methods proceed step down, faster, and with higher yields under the microwave irradiation (MWI) as compared with convection method. In many cases, reactions that normally require many hours at reflux temperature under normal conditions can be completed within several minutes or even seconds in a microwave oven, even at comparable reaction temperatures.[19] Quinoline synthesis has received much focus, and many methods have been developed for the synthesis, such as Skraup,[20] Doebner-Miller,[21] Pfitzinger,[22] and Friedlander.[23] Among all the methods, Friedlander annulation is one of the most popular methods for the substituted quinoline synthesis.[24–27] Recently, several Lewis acids,[28] Bronsted acids, and microwave-assisted irradiation[28] were used in the synthesis of quinoline moiety. Friedlander synthesis is an acid-catalyzed condensation of active methylene carbonyl compound with α-amino carbonyl compounds.

The continuation of our research was aimed at current manuscript synthesis and biological evaluation of the title compounds for their future drug development. The potency of molecule is increased by using dual blocker hybridization strategy (Figure 1). Herein, we report an efficient and microwave-assisted synthesis of quinoline hybrid thiosemicarbazide derivatives from the reaction of ethyl 2,4-dimethylquinoline-3-carboxylate and N^4-alkyl and aryl thiosemicarbazides in the presence of glacial acetic acid under microwave irradiation (Scheme 1). Ethyl 2,4-dimethylquinoline-3-carboxylate has been synthesized via condensation between ethyl acetoacetate and α-amino acetophenone in presence of *p*-toluenesulfonic acid (*p*-TSA) under microwave irradiation. Biological evaluation of title compounds was carried out in various strains, after which we conducted molecular docking study and also ADME-Tox and pharmacophore modeling studies on the Schrödinger software.

2 | EXPERIMENTAL

2.1 | Methods and materials

All chemicals were purchased from commercial suppliers; isothiocyanates were purchased from Sigma-Aldrich (USA), and all chemicals were of analytical grade. The reaction progress was monitored by thin-layer chromatography (TLC) of Merck pre-coated silica gel 60 F254 aluminum sheets, further visualized by UV light. CEM microwave synthesizer (USA) was used for the synthesis. All products were characterized by their melting points and spectral data. Melting points were measured on an Optimelt MPA 100 melting point instrument, and FT-IR spectra were recorded on a Perkin Elmer FT-IR 377 spectrometer using KBr pellets in cm^{-1}. ^{1}H-NMR spectra were recorded on a Bruker AV 400 MHz spectrometer using DMSO-d_6 as a solvent, TMS as the internal reference and ^{13}C-NMR spectra were recorded on a Bruker AV 100 MHz Spectrometer using DMSO-d_6 as solvent. Mass spectra (MS) were recorded at Advion expression CMS (USA). Ethyl acetate is used as mobile phase, and electron spray ionization (ESI) is used as the ion source. Elemental analysis was performed on a CHN elemental analyzer.

2.1.1 | Synthesis of ethyl 2,4-dimethylquinoline-3-carboxylate (3)

To a mixture of ethyl acetoacetate (1.0 mmol), alpha-amino acetophenone (1.0 mmol) and catalytic amount of *p*-TSA were collected in ethanol (5 mL); this solution was irradiated under the microwave at 300 W for 4 minutes. The reaction progress was monitored on the TLC plate. After the completion of the reaction, the mixture was poured in ice-cold water, then extract with ethyl acetate (50 × 2 mL), and the organic layer passed over sodium sulfate, and the mixture was evaporated to dryness in vacuo. The crude product was further purified by column chromatography.

2.1.2 | General procedure for the synthesis of N^4-alkyl and aryl thiosemicarbazides (6a-6s)

A mixture of various alkyl or aryl isothiocyanate (0.1 mmol) and hydrazine hydrate (0.1 mmol) was stirred in ethanol (5 mL) for a few minutes. An intermediate product was synthesized by microwave irradiating at 300 W for 2 to 4 minutes. The reaction progress was monitored on the TLC plate. After the completion of the reaction, mixture was poured in ice-cold water and the solid precipitates were collected. The crude products were used for the next step without further purification. Intermediate products were synthesized by the above described method.

2.1.3 | General procedure for the synthesis of 2-(2,4-dimethylquinoline-3-carbonyl)-*N*-substituted hydrazinecarbothioamide (7a-7s)

Intermediate products N^4-alkyl and aryl thiosemicarbazide (**6a**-**6s**, 1.0 mmol), ethyl 2,4-dimethylquinoline-3-carboxylate (**3**, 1.0 mmol), and a few drops of glacial acetic acid were mixed in ethanol (10 mL) and stirred well for 1 minute. This reaction solution was heated under the microwave irradiation at 300 W with a total irradiation time of 3 to 8 minutes. Reaction progress was monitored on the TLC plate at 30-s time interval. After the completion of the reaction, the mixture was poured in ice-cold water and extracted with ethyl acetate (50 × 2 mL). The organic layer passed over sodium sulfate, and the solution was evaporated to dryness in vacuo. The crude product was further purified by column chromatography. Solid product was obtained as a final product (Scheme 1).

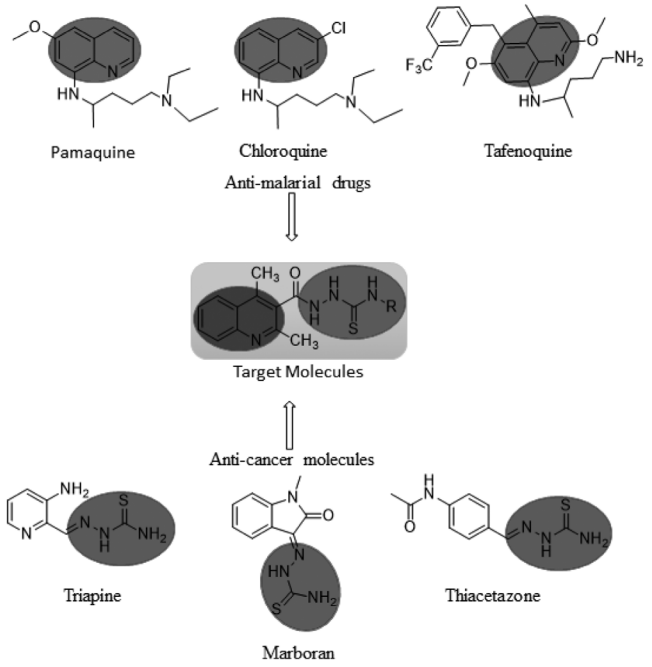

FIGURE 1 Dual blockers antimalarial drugs and anticancer molecules

2.2 | Spectral data

2.2.1 | 2,4-Dimethyl-*N*-((4-nitrophenyl) carbamothioyl)quinoline-3-carboxamide (7a)

Yellow solid; Yield: 70%; IR (KBr) λ_{max} (cm^{-1}): 3480, 3414 (NH), 1768 (C═O), 1617 (C═N), 1551 (C═S), 1132, 1086 (C—O); ^{1}H NMR (400 MHz, DMSO) δ: 11.22 (1H, s, —NH), 10.49 (1H, s, —NH), 8.60-8.50 (2H, d, Ar, J = 40), 8.09-8.08 (2H, dd, Ar, J = 4), 7.67-7.65 (1H, d, Ar, J = 8), 7.45-7.18 (3H, m, Ar), 3.74 (3H, s, —CH_3), 2.50 (3H, s, —CH_3); ^{13}C NMR (400 MHz, DMSO) δ: 166.37, 156.50, 147.75, 139.88, 139.17, 138.74, 131.78, 131.46, 130.77, 130.45, 129.89, 129.54, 128.33, 127.84, 127.62, 125.75, 125.42, 123.39, 121.13; Anal. Calcd for C, 59.99%; H, 4.24%; N, 14.73%; S, 8.43%; Found C, 59.89%; H, 4.28%; N, 14.77%; S, 8.44%; ESI-MS: m/z calculated 380.09, found $[M + H]^+$ 381.10.

2.2.2 | *N*-((4-Chlorophenyl) carbamothioyl)-2,4-dimethylquinoline-3-carboxamide (7b)

White solid; Yield: 83%; IR (KBr) λ_{max} (cm^{-1}): 3279, 3062 (NH), 1682 (C═O), 1588 (C═N), 1546 (C═S), 1148, 1078 (C—O); ^{1}H NMR (400 MHz, DMSO) δ: 10.99 (1H, s, —NH), 10.21 (1H, s, —NH), 8.48 (1H, d, Ar, J = 4), 7.80-7.64 (4H, m, Ar), 7.45-7.38 (3H, m, Ar), 2.73 (3H, s, —CH_3), 2.34 (3H, s, —CH_3); ^{13}C NMR (400 MHz, DMSO) δ: 156.49, 147.74, 138.75, 136.58, 131.77, 131.46, 130.76, 130.41, 129.88, 129.52, 128.79, 127.80, 127.61, 125.76, 123.40, 121.11; Anal. Calcd for C, 61.70%; H, 4.36%; N,

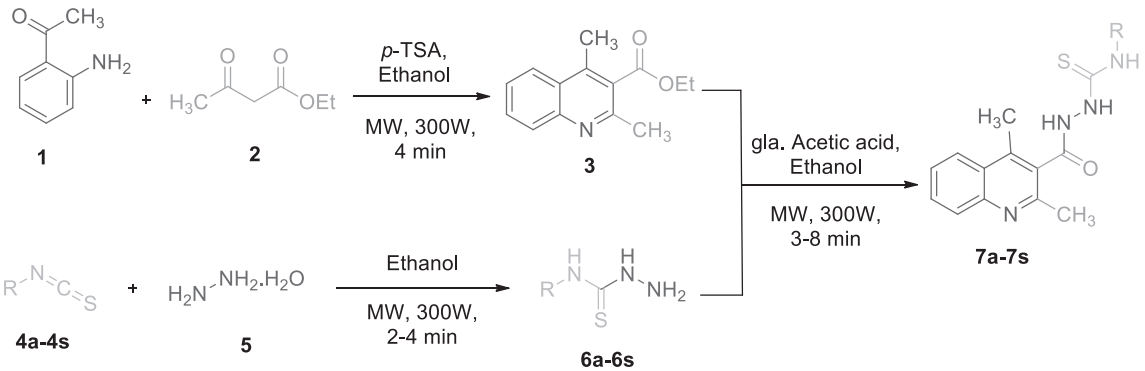

SCHEME 1 Microwave-assisted synthetic strategy for the target compounds (**7a-7s**)

11.36%; S, 8.67%; Found C, 61.68%; H, 4.39%; N, 11.40%; S, 8.61%; ESI-MS: m/z calculated 369.89, found $[M + H]^+$ 370.40.

2.2.3 | *N*-((4-Chlorophenyl) carbamothioyl)-2,4-dimethylquinoline-3-carboxamide (7c)

White solid; Yield: 76%; IR (KBr) λ_{max} (cm^{-1}): 3276 (NH), 1804 (C═O), 1594 (C═N), 1552 (C═S), 1152, 1085 (C—O); ^{1}H NMR (400 MHz, DMSO) δ: 10.83 (1H, s, —NH), 10.03 (1H, s, —NH), 8.50 (1H, d, Ar, $J = 4$), 8.09 (1H, d, Ar, $J = 4$), 7.80-7.78 (2H, dd, Ar, $J = 8$), 7.65-7.60 (2H, d, Ar, $J = 20$), 7.45-7.21 (2H, d, Ar, $J = 9.6$), 2.51 (3H, s, —CH_3), 2.35 (3H, t, —CH_3), 2.27 (3H, s, —CH_3); ^{13}C NMR (400 MHz, DMSO) δ: 166.15, 156.42, 147.78, 147.67, 139.88, 138.70, 131.80, 131.72, 131.46, 130.78, 130.62, 130.42, 130.11, 129.50, 127.77, 127.63, 127.42, 125.82, 123.45, 123.13, 120.96, 118.91; Anal. Calcd for C, 68.74%; H, 5.48%; N, 12.02%; S, 9.18%; Found C, 68.60%; H, 5.45%; N, 11.98%; S, 9.20%; ESI-MS: m/z calculated 349.45, found $[M + H]^+$ 350.50.

2.2.4 | 2,4-Dimethyl-*N*-(propylcarbamothioyl)quinoline-3-carboxamide (7d)

Off-white solid; Yield: 70%; IR (KBr) λ_{max} (cm^{-1}): 3209 (NH), 1778 (C═O), 1594 (C═N), 1533 (C═S), 1149, 1086 (C—O); ^{1}H NMR (400 MHz, DMSO) δ: 10.43 (1H, s, —NH), 8.61-7.67 (4H, m, Ar), 7.65-6.85 (4H, m, Ar), 3.73 (3H, s, —CH_3), 3.52 (3H, s, —CH_3), 2.50-1.90 (2H, m, —CH_2), 1.57 (3H, q, —CH_3); ^{13}C NMR (400 MHz, DMSO) δ: 156.47, 147.78, 138.71, 131.78, 131.45, 130.79, 130.45, 129.89, 129.55, 127.86, 127.63, 125.73, 123.38; Anal. Calcd for C, 63.76%; H, 6.35%; N, 13.94%; S, 10.64%; Found C, 63.60%; H, 6.29%; N, 13.90%; S, 10.61%; ESI-MS: m/z calculated 301.41, found $[M + H]^+$ 302.69.

2.2.5 | *N*-((3,4-Dichlorophenyl) carbamothioyl)-2,4-dimethylquinoline-3-carboxamide (7e)

White solid; Yield: 75%; IR (KBr) λ_{max} (cm^{-1}): 3195 (NH), 1678 (C═O), 1594 (C═N), 1513 (C═S), 1129, 1086 (C—O); ^{1}H NMR (400 MHz, DMSO) δ: 11.23 (1H, s, —NH), 10.29 (1H, s, —NH), 8.47 (1H, s, Ar), 8.09 (1H, d, Ar, $J = 4$), 7.80-7.78 (2H, dd, Ar, $J = 8$), 7.80-7.81 (1H, d, Ar, $J = 4$), 7.80-7.40 (3H, m, Ar), 2.59 (3H, s, —CH_3), 2.35 (3H, s, —CH_3); ^{13}C NMR (400 MHz, DMSO) δ: 156.56, 147.71, 139.52, 138.83, 131.74, 131.46, 130.78, 130.46, 129.86, 129.55, 128.86, 127.87, 127.62, 125.65, 123.32, 121.20; Anal. Calcd for C, 56.44%; H, 3.74%; N, 10.39%; S, 7.93%; Found C, 56.40%; H, 3.70%; N, 10.42%; S, 7.89%; ESI-MS: m/z calculated 403.03, found $[M + H]^+$ 404.10.

2.2.6 | *N*-(Tert-butylcarbamothioyl)-2,4-dimethylquinoline-3-carboxamide (7f)

Brown solid; Yield: 72%; IR (KBr) λ_{max} (cm^{-1}): 3480, 3414 (NH), 1785 (C═O), 1665 (C═N), 1593 (C═S), 1137, 1086 (C—O); ^{1}H NMR (400 MHz, DMSO) δ: 10.83 (1H, s, —NH), 10.03 (1H, s, —NH), 8.47 (1H, s, Ar), 8.60 (1H, d, Ar, $J = 4$), 7.80-7.78 (2H, dd, Ar, $J = 8$), 7.69-7.67 (2H, dd, Ar, $J = 8$), 7.18 (1H, d, Ar, $J = 4$), 3.36 (3H, s, —CH_3), 2.50 (3H, s, —CH_3), 2.30 (9H, s, —CH_3); ^{13}C NMR (400 MHz, DMSO) δ: 156.47, 147.77, 140.73, 138.71, 131.79, 131.45, 130.80, 130.46, 129.89, 129.55, 127.87, 127.40, 125.73, 123.37, 120.87; Anal. Calcd for C, 64.73%; H, 6.71%; N, 13.32%; S, 10.17%; Found C, 64.68%; H, 6.12%; N, 13.38%; S, 10.10%; ESI-MS: m/z calculated 315.14, found $[M + H]^+$ 317.25.

2.2.7 | *N*-(Benzylcarbamothioyl)-2,4-dimethylquinoline-3-carboxamide (7g)

White solid; Yield: 80%; IR (KBr) λ_{max} (cm^{-1}): 3285 (NH), 1789 (C═O), 1659 (C═N), 1551 (C═S), 1184, 1041 (C—O); ^{1}H NMR (400 MHz, DMSO) δ: 10.08 (1H, s, —NH), 9.09-9.07 (1H, d, Ar, $J = 8$), 8.43-8.36 (1H, d, Ar, $J = 28$), 7.50-7.46 (2H, dd, Ar, $J = 16$), 7.44-6.82 (4H, m, Ar), 4.88-4.79 (2H, d, —CH_2, $J = 36$), 2.88 (2H, s, —CH_3), 2.25 (3H, s, —CH_3), 1.94 (1H, s, —CH_3); ^{13}C NMR (400 MHz, DMSO) δ: 166.24, 156.50, 147.75, 139.80, 139.17, 138.73, 131.78, 131.46, 130.78, 130.46, 129.89, 129.54, 128.36, 127.85, 127.63, 126.56, 125.75, 125.47, 123.39, 121.14; Anal. Calcd for C, 68.74%; H, 5.48%; N, 12.02%; S, 9.18%; Found C, 68.69%; H, 5.45%; N, 11.98%; S, 9.14%; ESI-MS: m/z calculated 349.12, found $[M + H]^+$ 350.30.

2.2.8 | *N*-((4-Methoxyphenyl) carbamothioyl)-2,4-dimethylquinoline-3-carboxamide (7h)

Light brown solid; Yield: 81%; IR (KBr) λ_{max} (cm^{-1}): 3397 (NH), 1819 (C═O), 1671 (C═N), 1550 (C═S), 1130, 1086 (C—O); ^{1}H NMR (400 MHz, DMSO) δ: 11.22 (1H, s, —NH), 9.55 (1H, s, —NH), 8.61-7.85 (4H, m, Ar), 7.71-6.90 (4H, m, Ar), 3.74 (3H, s, —OCH_3), 2.50 (3H, s, —CH_3), 1.30 (3H, s, —CH_3); ^{13}C NMR (400 MHz, DMSO)

δ: 156.57, 147.72, 138.82, 135.89, 132.91, 132.57, 131.74, 131.47, 130.77, 130.45, 129.87, 129.55, 128.95, 127.85, 127.61, 125.67, 123.34, 121.23; Anal. Calcd for C, 65.73%; H, 5.24%; N, 11.50%; S, 8.77%; Found C, 65.67%; H, 5.20%; N, 11.45%; S, 8.71%; ESI-MS: m/z calculated 365.12, found $[M + H]^+$ 367.81.

2.2.9 | *N*-((4-Iodophenyl)carbamothioyl)-2,4-dimethylquinoline-3-carboxamide (7i)

Light brown solid; Yield: 76%; IR (KBr) λ_{max} (cm^{-1}): 3351, 3274 (NH), 1777 (C═O), 1596 (C═N), 1553 (C═S), 1120, 1088 (C—O); ^{1}H NMR (400 MHz, DMSO) δ: 11.00 (1H, s, —NH), 10.19 (1H, s, —NH), 8.48-7.06 (8H, m, Ar), 2.89 (3H, s, —CH_3), 2.27 (S, 3H, —CH_3); ^{13}C NMR (400 MHz, DMSO) δ: 166.38, 156.52, 147.69, 138.79, 131.75, 131.48, 130.76, 130.41, 129.87, 129.51, 127.80, 127.61, 125.71, 125.48, 123.35, 120.83, 120.45; Anal. Calcd for C, 49.47%; H, 3.50%; N, 9.11%; S, 6.95%; Found C, 49.40%; H, 3.48%; N, 9.08%; S, 6.89%; ESI-MS: m/z calculated 461.01, found $[M + H]^+$ 462.68.

2.2.10 | *N*-((3,5-Dichlorophenyl) carbamothioyl)-2,4-dimethylquinoline-3-carboxamide (7j)

White solid; Yield: 76%; IR (KBr) λ_{max} (cm^{-1}): 3335, 3156 (NH), 1659 (C═O), 1592 (C═N), 1546 (C═S), 1157, 1088 (C—O); ^{1}H NMR (400 MHz, DMSO) δ: 11.19 (1H, s, —NH), 10.31 (1H, s, —NH), 8.47-6.85 (8H, m, Ar), 2.22 (3H, s, —CH_3), 2.14 (3H, s, —CH_3); ^{13}C NMR (400 MHz, DMSO) δ: 156.47, 147.77, 140.79, 138.70, 131.79, 131.44, 130.80, 130.47, 130.10, 129.98, 129.56, 127.88, 127.64, 125.72, 123.36, 120.88; Anal. Calcd for C, 56.44%; H, 3.74%; N, 10.39%; S, 7.93%; Found C, 56.41%; H, 3.79%; N, 10.29%; S, 7.87%; ESI-MS: m/z calculated 403.31, found $[M + H]^+$ 406.32.

2.2.11 | *N*-((2-Methoxyphenyl) carbamothioyl)-2,4-dimethylquinoline-3-carboxamide (7k)

White solid; Yield: 70%; IR (KBr) λ_{max} (cm^{-1}): 3362 (NH), 1817 (C═O), 1661 (C═N), 1535 (C═S), 1143, 1056 (C—O); 1H NMR (400 MHz, DMSO) δ: 11.23 (1H, s, —NH), 10.08 (1H, s, —NH), 8.43-6.94 (8H, m, Ar), 3.81 (3H, s, —OCH_3), 2.51 (3H, s, —CH_3), 2.34 (3H, s, —CH_3); ^{13}C NMR (400 MHz, DMSO) δ: 147.72, 138.78, 131.74, 131.45, 130.77, 130.44, 129.86, 129.55, 128.95, 127.85, 127.61, 125.67, 123.33, 121.19; Anal. Calcd for C, 65.73%; H, 5.24%; N, 11.50%; S, 8.77%; Found C, 65.69%; H, 5.20%; N, 11.48%; S, 8.71%; ESI-MS: m/z calculated 365.12, found $[M + H]^+$ 366.87.

2.2.12 | *N*-((3-Methoxyphenyl) carbamothioyl)-2,4-dimethylquinoline-3-carboxamide (7l)

White solid; Yield: 82%; IR (KBr) λ_{max} (cm^{-1}): 3435 (NH), 1763 (C═O), 1668 (C═N), 1548 (C═S), 1131, 1087 (C—O); ^{1}H NMR (400 MHz, DMSO) δ: 11.05 (1H, s, —NH), 10.92 (1H, s, —NH), 8.50-6.75 (8H, m, Ar), 2.50 (S, 3H, CH_3), 3.76 (S, 3H, OCH_3); ^{13}C NMR (400 MHz, DMSO) δ: 159.60, 148.48, 147.76, 138.71, 134.46, 131.93, 131.85, 131.72, 131.46, 131.25, 130.73, 130.37, 130.28, 129.84, 129.81, 129.45, 128.73, 128.39, 128.16, 127.63, 126.59, 125.48, 121.95, 119.44; Anal. Calcd for C, 65.73%; H, 5.24%; N, 11.50%; S, 8.77%; Found C, 65.60%; H, 5.20%; N, 11.30%; S, 8.70%; ESI-MS: m/z calculated 365.12, found $[M + H]^+$ 366.87.

2.2.13 | 2,4-Dimethyl-*N*-((3,4,5-trichlorophenyl)carbamothioyl) quinoline-3-carboxamide (7m)

White solid; Yield: 80%; IR (KBr) λ_{max} (cm^{-1}): 3197 (NH), 1668 (C═O), 1595 (C═N), 1546 (C═S), 1131, 1086 (C—O); ^{1}H NMR (400 MHz, DMSO) δ: 10.43 (1H, s, —NH), 10.05 (1H, s, —NH), 8.48-7.05 (8H, m, Ar), 2.28 (3H, s, —CH_3), 2.01 (3H, s, —CH_3); ^{13}C NMR (400 MHz, DMSO) δ: 166.34, 156.49, 147.71, 138.77, 131.76, 131.48, 130.77, 130.41, 129.88, 129.50, 127.77, 127.61, 125.74, 123.38, 120.84; Anal. Calcd for C, 52.01%; H, 3.22%; N, 9.58%; S, 7.31%; Found C, 51.93%; H, 3.20%; N, 9.51%; S, 7.24%; ESI-MS: m/z calculated 436.99, found $[M + H]^+$ 438.21.

2.2.14 | *N*-((2,4-Dichlorophenyl) carbamothioyl)-2,4-dimethylquinoline-3-carboxamide (7n)

White solid; Yield: 74%; IR (KBr) λ_{max} (cm^{-1}): 3125 (NH), 1801 (C═O), 1638 (C═N), 1523 (C═S), 1159, 1086 (C—O); ^{1}H NMR (400 MHz, DMSO) δ: 11.17 (1H, s, —NH), 10.11 (1H, s, —NH), 8.45-6.68 (8H, m, Ar), 2.51 (3H, s, —CH_3), 2.27 (3H, s, —CH_3); ^{13}C NMR (400 MHz, DMSO) δ: 156.49, 147.73, 138.75, 136.59, 131.78, 131.45, 130.77, 130.42, 129.88, 129.52, 128.80, 127.81, 127.62, 125.76, 123.40, 121.11; Anal. Calcd for C, 56.44%; H, 3.74%; N, 10.39%; S, 7.93%; Found C, 56.37%; H, 3.61%; N, 10.34%; S, 7.89%; ESI-MS: m/z calculated 403.31 found $[M + H]^+$ 406.32.

2.2.15 | *N*-((2,4-Difluorophenyl) carbamothioyl)-2,4-dimethylquinoline-3-carboxamide (7o)

Greenish solid; Yield: 83%; IR (KBr) λ_{max} (cm^{-1}): 3420, 3224 (NH), 1785 (C═O), 1613 (C═N), 1550 (C═S), 1130, 1088 (C—O); ^{1}H NMR (400 MHz, DMSO) δ: 11.08 (1H, s, —NH), 10.04 (1H, s, —NH), 8.49-6.86 (8H, m, Ar), 2.51 (3H, s, —CH_3), 2.25 (3H, s, —CH_3); ^{13}C NMR (400 MHz, DMSO) δ: 167.71, 164.34, 156.33, 147.79, 139.91, 138.52, 133.22, 131.89, 131.86, 131.37, 130.86, 130.59, 130.14, 129.58, 128.84, 128.53, 127.99, 127.69, 125.58, 123.32, 120.86; Anal. Calcd for C, 61.44%; H, 4.07%; N, 11.31%; S, 8.63%; Found C, 61.36%; H, 4.01%; N, 11.30%; S, 8.64%; ESI-MS: *m*/*z* calculated 371.09, found $[M + H]^+$ 372.09.

2.2.16 | *N*-(Ethylcarbamothioyl)-2,4-dimethylquinoline-3-carboxamide (7p)

White solid; Yield: 79%; IR (KBr) λ_{max} (cm^{-1}): 3243 (NH), 1773 (C═O), 1668 (C═N), 1544 (C═S), 1127, 1088 (C—O); ^{1}H NMR (400 MHz, DMSO) δ: 11.04 (1H, s, —NH), 10.11 (1H, s, —NH), 7.80-7.20 (4H, m, Ar), 3.37 (2H, q, ehtyl-CH_2), 2.50 (3H, s, —CH_3), 2.34 (3H, s, —CH_3); ^{13}C NMR (400 MHz, DMSO) δ: 156.82, 156.51, 147.73, 138.87, 131.78, 131.77, 131.46, 130.76, 130.41, 129.87, 129.52, 127.80, 127.61, 125.77, 123.41, 121.13, 113.54; Anal. Calcd for C, 62.69%; H, 5.96%; N, 14.62%; S, 11.16%; Found C, 62.69%; H, 5.89%; N, 14.63%; S, 11.11%; ESI-MS: *m*/*z* calculated 287.11, found $[M + H]^+$ 288.36.

2.2.17 | 2,4-Dimethyl-*N*-(phenylcarbamothioyl)quinoline-3-carboxamide (7q)

White solid; Yield: 78%; IR (KBr) λ_{max} (cm^{-1}): 3318, 3298 (NH), 1784 (C═O), 1664 (C═N), 1546 (C═S), 1130, 1087 (C—O); ^{1}H NMR (400 MHz, DMSO) δ: 10.75 (1H, s, —NH), 10.15 (1H, s, —NH), 8.50-7.21 (9H, m, Ar), 2.35 (3H, s, —CH_3), 2.28 (3H, s, —CH_3); ^{13}C NMR (400 MHz, DMSO) δ: 165.57, 155.46, 146.11, 140.10, 139.20, 138.45, 131.60, 131.50, 130.45, 130.35, 129.45, 129.23, 128.13, 127.75, 127.41, 125.45, 125.21, 123.12, 121.45; Anal. Calcd for C, 68.03%; H, 5.11%; N, 12.53%; S, 9.56%; Found C, 67.98%; H, 5.08%; N, 12.48%; S, 9.50%; ESI-MS: *m*/*z* calculated 335.42, found $[M + H]^+$ 336.83.

2.2.18 | *N*-(Cyclohexylcarbamothioyl)-2,4-dimethylquinoline-3-carboxamide (7r)

White solid; Yield: 74%; IR (KBr) λ_{max} (cm^{-1}): 3417, 3154 (NH), 1724 (C═O), 1633 (C═N), 1619, 1582 (C═S), 1371 (C═S), 1125, 1099 (C—O); ^{1}H NMR (400 MHz, DMSO) δ: 10.48 (1H, s, —NH), 8.31 (1H, s, —NH), 7.83-7.38 (4H, m, Ar), 4.21-4.20 (1H, s, cyclohexyl), 2.51 (3H, s, —CH_3), 2.20 (3H, s, —CH_3), 1.90-1.13 (m, 10H, cyclohexyl); ^{13}C NMR (400 MHz, DMSO) δ: 166.12, 156.47, 147.47, 139.21, 139.01, 138.47, 131.38, 131.33, 130.64, 130.32, 129.59, 129.24, 128.34, 127.75, 127.32, 125.68, 125.41, 123.40, 121.68; Anal. Calcd for C, 66.83%; H, 6.79%; N, 12.31%; S, 9.39%; Found C, 66.80%; H, 6.81%; N, 12.27%; S, 9.34%; ESI-MS: *m*/*z* calculated 341.16, found $[M + H]^+$ 342.96.

2.2.19 | *N*-Carbamothioyl-2,4-dimethylquinoline-3-carboxamide (7s)

White solid; Yield: 78%; IR (KBr) λ_{max} (cm^{-1}): 3410, 3366 (NH), 1784 (C═O), 1639 (C═N), 1526 (C═S), 1114, 1088 (C—O); ^{1}H NMR (400 MHz, DMSO) δ: 10.49 (1H, s, —NH), 8.47 (2H, s, —NH_2), 7.99-7.38 (4H, m, Ar), 2.51 (3H, s, —CH_3), 2.26 (3H, s, —CH_3); ^{13}C NMR (400 MHz, DMSO) δ: 165.01, 154.87, 147.45, 139.12, 139.01, 138.65, 131.84, 131.23, 130.67, 130.35, 129.78, 129.64, 128.34, 127.68, 127.40, 125.98, 125.46, 123.63, 121.74; Anal. Calcd for C, 60.21%; H, 5.05%; N, 16.20%; S, 12.36%; Found C, 60.19%; H, 5.01%; N, 16.11%; S, 12.29%; ESI-MS: *m*/*z* calculated 259.08, found $[M + H]^+$ 260.64.

3 | BIOLOGICAL ASSAY

3.1 | In-vitro antibacterial and antifungal activity

The all newly synthesized compounds (**7a-7s**) were evaluated for their antibacterial activity using the Gram-positive and Gram-negative strains. Two strains of Gram-positive bacteria (*Staphylococcus aureus* MTCC 96 and *Streptococcus pyogenes* MTCC 442) and two strains of Gram-negative bacteria (*Escherichia coli* MTCC 443 and *Pseudomonas aeruginosa* MTCC 1688) as well as three fungal strains (*Aspergillus clavatus* MTCC 1323, *Candida albicans* MTCC 227, and *Aspergillus niger* MTCC 282) by using the reported agar dilution method.[28] Ciprofloxacin, ampicillin, and chloramphenicol were used as a standard drug for the antibacterial activity, and greseofulvin and nystatin were used as a standard drug for the antifungal activity.

3.2 | In-vitro antimalarial and antituberculosis activity

The title compounds (**7a-7s**) were evaluated in in-vitro antimalarial activity as per the reported method against

the *Plasmodium falciparum* strain[29] and in-vitro anti-tuberculosis activity as per the reported method against the *H37RV* strain.[30] Graphical presentation of biological activity is shown in a Figure 2.

4 | COMPUTATIONAL STUDY

4.1 | Molecular docking

The potential binding mode and the binding interaction of the ligand with *P. falciparum* dihydrofolate reductase thymidylate synthase *PFDHFR-TS* have been investigated by using Maestro 11.0 Schrödinger, LLC, New York, NY, 2018. The 3D structures of all the compounds were generated via using Marvin suites and saved as SDF file. The 3D crystal structures of *PFDHFR-TS* from malarial (PDB ID: *3JSU*, *4DP3*, *1J3K*) were retrieved from the protein data bank (www.rcsb.org). The protein was selected on the basis of structural similarity of ligands, resolution, and expression system. Moreover, the selected protein (*pf*-strain) is encouraging us to do the docking in the active site for the better understanding of interaction. The ligands with the lowest energy, correct Lewis structure, tautomers, and ionization states (pH 7.0 ± 2.0) for each of the ligands were generated and optimized with default settings and were prepared for molecular docking using LigPrep module of Schrödinger. The OPLS_2005[31–33] force field was used for computing partial atomic charges. The proteins were prepared for docking using a protein preparation wizard module in Maestro. Bond order and formal charges were assigned, and hydrogen atoms were added to the crystal structure. Further refinement of the structure OPLS_2005 force field parameter was used to alleviate steric clashes. The receptor grid was generated using Glide 5.8 (Maestro Schrödinger, LLC, New York, NY, 2018) with default settings for all parameters. An approximately large grid size was preferred to include all active site residues involved in substrate binding. The glide extra-standard precision (XP) mode was used for docking of the generated receptor grid file along with all prepared ligand conformers. Default settings were retained for the scoring and refinement.

4.2 | ADME-Tox study

A set of ADME-Tox-related properties of the synthesized compounds were predicted by using a Qikpro program (Schrödinger, LLC, New York, NY, 2018).[34] LigPrep module was used to prepare the compounds and utilized for the calculation of pharmacokinetic parameters by Qikpro module. The program Qikpro generates physically

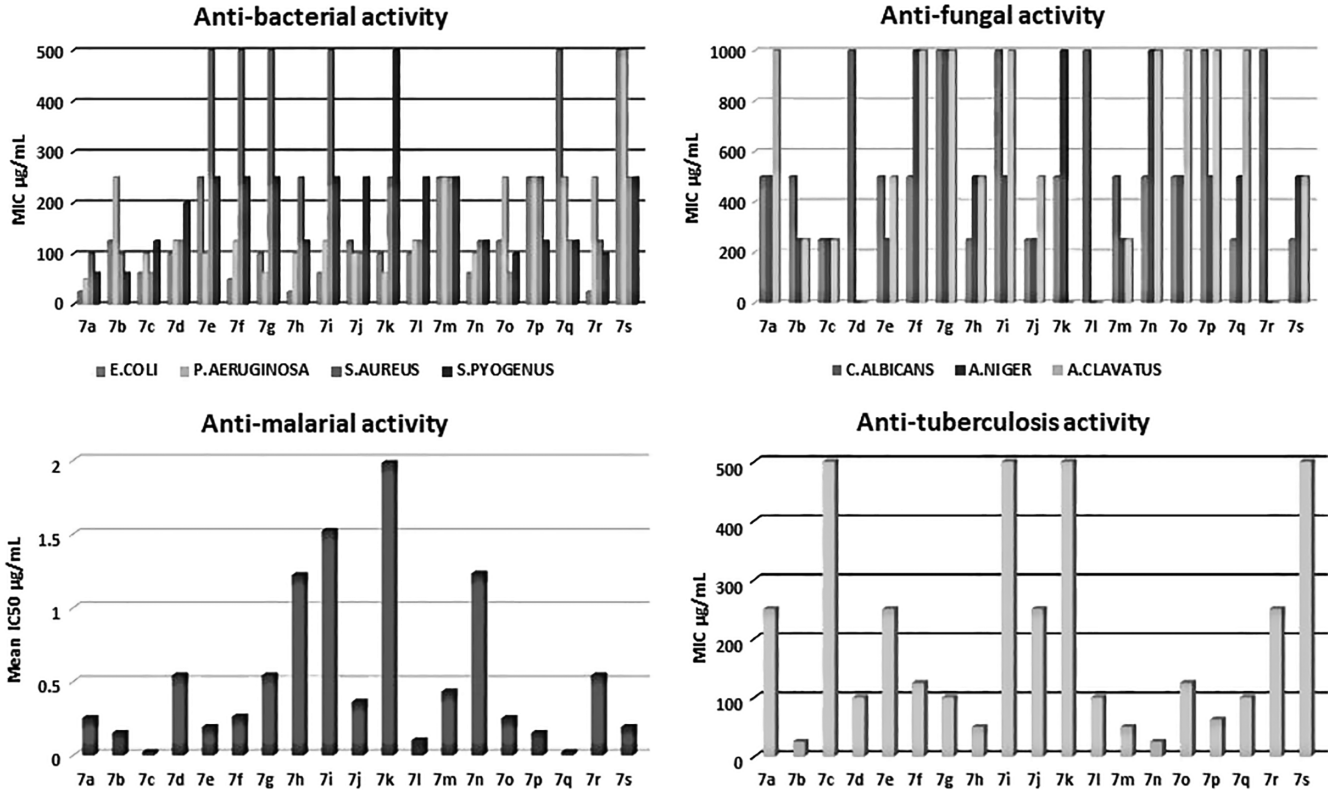

FIGURE 2 Graphical presentation of biological activity

relevant descriptors and uses them to perform ADME-Tox predictions and utilizes the method of Jorgensen to calculate pharmacokinetic properties and descriptors.

4.3 | Molecular dynamics

The natural dynamics on different timescales of a docked complex of compound **7e** and protein (PDB: *3JSU*) and the thermal average of the molecular properties of the complex are carried with the help of molecular dynamics (MD) stimulation. MD simulations have been conducted by Desmond program,[35,36] as implemented Schrödinger Materials Science Suite 2015-4.[34] OPLS_2005 force field with NPT ensemble class have been used, while pressure and temperature were set to 1.0325 bar and 300 K, respectively. The system was modeled by placing one **7e** molecule into the cubic box with around 3000 water molecules, and the simulation time was set to 10 ns, cut-off radius was set to 12 Å, pressure was set to 1.0325 bars, and the temperature was set to 300 K. In all cases when Desmond was used, input and output files were manipulated by Maestro graphical user interface application of Schrödinger Materials Science Suite 2018.

4.4 | Pharmacophore model

4.4.1 | Dataset pool

A pool of 19 molecules dataset were prepared in LigPrep module, the addition of hydrogen and generation of conformers at 7.0 P^H using OPLS 2005 force field (LigPrep, Schrödinger, LLC, New York, NY, 2018).[34] Phase module implemented in the Maestro 11.0 software package (Schrodinger, LLC) was used to generate pharmacophore models.

4.4.2 | Pharmacophore modeling and validation

For alignment, the compounds from the dataset were docked into the active site pocket of the crystal structure of *3JSU*, *4DP3*, and *1J3K*. Phase module was used for the pharmacophore generation (Phase, version 3.3, Schrödinger, LLC, New York, NY, 2018). The dataset compounds were divided as low, moderate, and high actives. Low active molecules were selected as inactive groups, and highly active compounds were selected

TABLE 1 Microwave-assisted synthesis of quinoline hybrid thiosemicarbazide derivatives (**7a-7s**)

			MWI	
Entry	**Product Code**	**R**	**Time, min**	**Yield, %[a]**
1	**7a**	4-$NO_2C_6H_5$	3	70
2	**7b**	4-ClC_6H_5	5	83
3	**7c**	4-$CH_3C_6H_5$	5	76
4	**7d**	Isopropyl	8	70
5	**7e**	3,4-diClC_6H_4	5	75
6	**7f**	*t*-butyl	8	72
7	**7g**	—$CH_2C_6H_5$	5	80
8	**7h**	4-$OCH_3C_6H_5$	5	81
9	**7i**	4-IC_6H_5	5	76
10	**7j**	3,5-diClC_6H_4	5	76
11	**7k**	2-$OCH_3C_6H_5$	5	70
12	**7l**	3-$OCH_3C_6H_5$	5	82
13	**7m**	3,4,5-triClC_6H_2	5	80
14	**7n**	2,4-diClC_6H_4	5	74
15	**7o**	2,4-diFC_6H_4	5	83
16	**7p**	Ethyl	8	79
17	**7q**	C_6H_5	3	78
18	**7r**	C_6H_{11}	5	74
19	**7s**	H	5	78

[a]Purified yield.

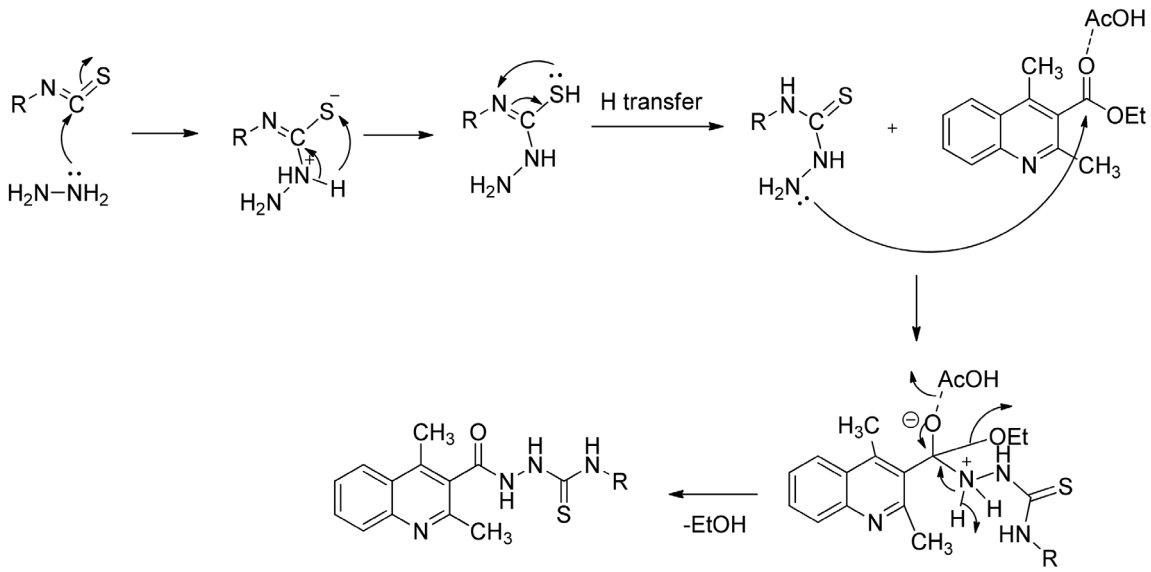

SCHEME 2 Proposed reaction mechanism

as active groups. For pharmacophore sites, a default feature was selected with acceptor (A), donor (D), hydrophobic (H), negative (N), positive (P), and aromatic ring (R). This feature was used in the clustering and rescoring of the models. The parameters include (a) survival score, which measures the quality of alignment of the particular pharmacophore model, and (ii) site score is an indication of how closely the site points are superimposed in an alignment to the pharmacophore of the structures that contribute to the hypothesis.

5 | RESULTS AND DISCUSSION

The reaction sequences employed for the synthesis of the title compounds (**7a-7s**) are shown in Scheme 1. Ethyl 2,4-dimethylquinoline-3-carboxylate (**3**) is readily prepared according to previously reported methods, in which cyclization occurred by the ethyl acetoacetate, α-amino acetophenone in ethanol under the microwave irradiation (MWI) at 300 W (130°C), and the key intermediate N^4-alkyl and aryl thiosemicarbazides (**6a-6s**) were synthesized also prepared according to previously reported method [A], in which hydrazine hydrate was added in to various isothiocyanates in the ethanol under the microwave irradiation (MWI) at 300 W. The final novel derivatives of substituted quinolines (**7a-7s**) were synthesized in presence of glacial acetic acid under the microwave irradiation at 300 W. Finally, targeted compounds, 2-(2,4-dimethylquinoline-3-carbonyl)-*N*-substituted hydrazinecarbothioamide were obtained in 83% to 70% yields with high purity within 3 to 8 minutes at the 300-W microwave irradiation. Aliphatic substitution **7d**, **7f**, and **7p** (Table 1, entries 4, 6, and 16) were obtained in the lower yield, and **7b**, **7c**, **7h**, and **7q** (Table 1, entries 2, 3, 8, and 17) were obtained in the higher yield. The structures of novel synthesized compounds were confirmed by FTIR, ^{1}H NMR, and ESI-MS and elemental analysis. We have also proposed a mechanism for the novel synthesized derivatives, which is shown in Scheme 2.

The formation of final molecules of the IR spectrum showed a strong band at a range of 1700, 1600, and 3400 cm^{-1} represented the presence of carbonyl, C═C, and —NH— groups in the molecules, respectively. ^{1}H NMR spectrum showed two peaks at a range of 11 to 10 ppm, indicating the 2 hydrogen of —NH— group of thiosemicarbazide, and a multi-plate peak at a range of 2 to 3 ppm, indicating the 6 hydrogen of two methyl groups of substituted quinoline.

5.1 | Biology

5.1.1 | In-vitro antibacterial and antifungal activity

Reviewing the biological activities of quinoline hybrid thiosemicarbazide derivatives indicates all the scaffolds were found to be highly potent to moderate activity against the specific strains. Table 2 shows that bioassay results of a series of **7a-7s** compounds relevant that compound **7a** (MIC 50 μg/mL) containing nitro group at 4-position of phenyl ring was found to be the most potent

against the *P. aeruginosa* as compared with chloramphenicol (MIC 50 μg/mL) as a standard drug, while compounds **7g** and **7k** (62.5 μg/mL) exhibited more potent activity against the *P. aeruginosa*. However, compounds **7d**, **7f** (MIC 125 μg/mL), and **7p** (MIC 100 μg/mL), having aliphatic linker, show the minimum inhibition concentration with the lowest value in *P. aeruginosa* strain (Table 2, entries 4, 6, and 16). Chloro-substituted group on phenyl ring compounds **7e**, **7j** (100 μg/mL) and **7b**, **7m** (MIC 250 μg/mL) display excellent activity on the same strain, and compound **7o** (250 μg/mL) containing fluoro group at 2-position and 4-position of the phenyl ring was found to be the most active compound against the *P. aeruginosa* compared with chloramphenicol and

TABLE 2 In vitro biological activity of title compounds **7a-7s**

		Antibacterial								
		Gram-Negative Organism[a]		**Gram-Positive Organism[b]**		**Antifungal[c]**			**Antimalaria[d]**	**AntiTB[e]**
Entry	**Pro. Code**	***Ec***	***Pa***	***Sa***	***Sp***	***Ca***	***An***	***Ac***	***Pf***	***H37RV***
1	**7a**	25	50	100	62.5	500	500	1000	0.25	250
2	**7b**	125	250	100	62.5	500	250	250	0.15	25
3	**7c**	62.5	100	62.5	125	250	250	250	0.02	500
4	**7d**	100	125	125	200	1000	>1000	>1000	0.54	100
5	**7e**	250	100	500	250	500	250	500	0.19	250
6	**7f**	50	125	500	250	500	1000	1000	0.26	125
7	**7g**	100	62.5	500	250	1000	1000	1000	0.54	100
8	**7h**	25	100	250	125	250	500	500	1.22	50
9	**7i**	62.5	125	500	250	1000	500	1000	1.52	500
10	**7j**	125	100	100	250	250	250	500	0.36	250
11	**7k**	100	62.5	250	500	500	1000	>1000	1.98	500
12	**7l**	100	125	125	250	1000	>1000	>1000	0.10	100
13	**7m**	250	250	250	250	500	250	250	0.43	50
14	**7n**	62.5	100	125	125	500	1000	1000	1.23	25
15	**7o**	125	250	62.5	100	500	500	1000	0.25	125
16	**7p**	250	250	250	125	1000	500	1000	0.15	62.5
17	**7q**	500	250	125	125	250	500	1000	0.02	100
18	**7r**	25	250	125	100	1000	>1000	>1000	0.54	250
19	**7s**	500	500	250	250	250	500	500	0.19	500
20	**Amp**[f]	100	—	250	100	—	—	—	—	—
21	**Cam**[f]	50	50	50	50	—	—	—	—	—
22	Cipro[f]	25	25	50	50	—	—	—	—	—
23	**Ny**[f]	—	—	—	—	100	100	100	—	—
24	**Gris**[f]	—	—	—	—	500	100	100	—	—
25	**INH**[f]	—	—	—	—	—	—	—	—	0.20
26	**RMP**[f]	—	—	—	—	—	—	—	—	1.00
27	**Quin**[f]	—	—	—	—	—	—	—	0.26	—
28	**CQ**[f]	—	—	—	—	—	—	—	0.02	—

Note: —, not tested.

[a]Values expressed in μg/mL, *Escherichia coli* MTCC 443 (*Ec*), *Pseudomonas aeruginosa* MTCC 1688 (*Pa*).

[b]Values expressed in μg/mL, *Staphylococcus aureus* MTCC 96 (*Sa*), *Streptococcus pyogenes* MTCC 442 (*Sp*).

[c]Values expressed in μg/mL, *Candida albicans* MTCC 227 (*Ca*), *Aspergillus niger* MTCC 282 (*An*), *Aspergillus clavatus* MTCC 1323 (*Ac*).

[d]Values expressed in IC50 μg/mL, *Plasmodium falciparum*.

[e]Values expressed in MIC μg/mL, H37RV strain.

[f]Standard drug (Ampicillin, Chloramphenicol, Ciprofloxacin, Nystatin, Griseofulvin, Isoniazid, Rifampicin, Quinine, Chloroquine).

ciprofloxacin as standard drug. Compounds **7a**, **7h** (MIC 25 μg/mL) at fourth substitution at phenyl ring and **7r** (MIC 25 μg/mL) with a cyclo group having excellent activity against the *E. coli* compared with ciprofloxacin (MIC 25 μg/mL). Compound **7f** (MIC 50 μg/mL), having aliphatic linkage (*t*-butyl group), has good potency against the *E. coli* as compared with chloramphenicol (MIC 50 μg/mL) as standard drug. Here, compounds **7c, 7i,** and **7n** (MIC 62.5 μg/mL) exhibited high activity against the *E. coli* as compared with ampicillin as standard drug. Compound **7c** (MIC 62.5 μg/mL) having a methyl group at 4-position and **7o** (MIC 62.5 μg/mL) having fluorine group shows high potency against the *S. aureus*. Compounds **7a**, **7b**, and **7j** (MIC 100 μg/mL) have good potency against the *S. aureus* as compared with ampicillin (250 μg/mL) standard drug. Compounds **7c**, **7h**, **7j**, **7q**, and **7s** (MIC 250 μg/mL) show good activity against the *C. albicans*, compounds **7b**, **7c**, **7e**, **7j**, and **7m** (MIC 250 μg/mL) show good activity against *A. niger*, and compounds **7b**, **7c**, and **7m** (MIC 250 μg/mL) shows good activity against the *A. clavatus*. Moreover, other remaining compounds exhibited moderate activity against the bacterial and fungal strains.

5.1.2 | In-vitro antimalarial and antituberculosis activity

The antimalarial activity was performed against *P. falciparum* strain by the reported method (see Supporting Information). Results show that compounds **7a, 7b, 7c, 7e, 7f, 7l, 7o, 7p, 7q**, and **7s** exhibited higher potency activity against the *P. falciparum* strain. Compound **7a** (0.25 μg/mL) having a nitro group at 4-position on phenyl, **7f** (0.25 μg/mL) having *t*-butyl linkage, and **7o** (0.26 μg/mL) having fluorine at 2,4-position phenyl exhibited excellent activity against the *P. falciparum* as compared with quinine (0.26 μg/mL). Compound **7b** (0.15 μg/mL) containing chlorine at 4-position and **7p** (0.15 μg/mL) containing aliphatic linkage exhibited excellent activity as compared with quinine. Compound **7c** (0.02 μg/mL) containing methyl group at 4-position on phenyl and **7q** (0.02 μg/mL) having cyclo phenyl group shows higher activity than other compounds

TABLE 3 XP Glide score for compounds **7a**-**7s** with *PFDHFR-TS*

		PDB:*3JSU*		**PDB:4DP3**		**PDB:1J3K**	
Entry	**Product Code**	**XP GScore**	**XP HBond**	**XP GScore**	**XP HBond**	**XP GScore**	**XP HBond**
1	7a	−7.008	−0.194	−6.114	−0.448	−2.048	0
2	7b	−8.38	−1.33	−5.828	−0.84	−4.323	−0.29
3	7c	−8.292	−0.649	−7.239	−0.746	−3.324	−0.368
4	7d	−6.77	0	−6.245	−0.645	−3.521	−0.7
5	7e	−9.592	−0.368	−6.488	−0.343	−3.892	−0.7
6	7f	−7.381	−0.002	−5.432	−0.659	−3.696	−0.376
7	7 g	−7.938	−1.27	−6.234	−0.57	−3.403	−0.53
8	7h	−8.188	−0.622	−6.642	−0.465	−3.874	−0.576
9	7i	−8.823	0	−6.044	−0.879	−3.035	−0.7
10	7j	−7.365	−1.627	−5.978	0	−2.546	0
11	7 k	−7.669	−0.225	−6.473	0	−2.225	−0.448
12	7l	−6.12	−0.814	−5.822	0	−3.039	−0.994
13	7 m	−5.894	−0.453	−6.225	−0.281	−3.48	0
14	7n	−8.649	0	−6.285	−0.295	−3.236	−0.782
15	7o	−8.375	−0.7	−6.508	−0.817	−3.549	−0.15
16	7p	−5.38	−0.468	−5.444	−0.123	−3.038	−0.796
17	7q	−8.453	−0.556	−6.965	−0.971	−1.987	−0.992
18	7r	−8.331	−1.007	−4.609	−0.418	−2.537	−0.7
19	7s	−6.628	−0.759	−5.236	−0.04	−3.963	−0.369
20	**Quin***	−4.899	−0.645	−6.273	−0.7	−3.907	0
21	**CQ***	−5.568	0	−6.675	−0.9	−3.781	0

as compared with standard drugs quinine (0.26 μg/mL) and chloroquine (0.02 μg/mL). Compounds **7e** (0.19 μg/mL), **7l** (0.10 μg/mL), and **7s** (0.19 μg/mL) show good activity compared with quinine as a standard drug. Other remaining compounds also show a moderated activity with reference to standard drugs. The anti *Mycobacterium tuberculosis* activity performed against the *H37RV* strain by the broth dilution method. Results show that compounds **7b** and **7n** having chlorine group at 4-position and 2, 4 di chloro group on the phenyl ring exhibited excellent activity against the *H37RV* strain with MIC value 25 μg/mL. Compound **7h** has the methoxy group at 4-position on phenyl ring, and compound **7m** having chlorine group shows potent activity against the same strain with MIC 50 μg/mL. In addition, other remaining molecules did not produce significant

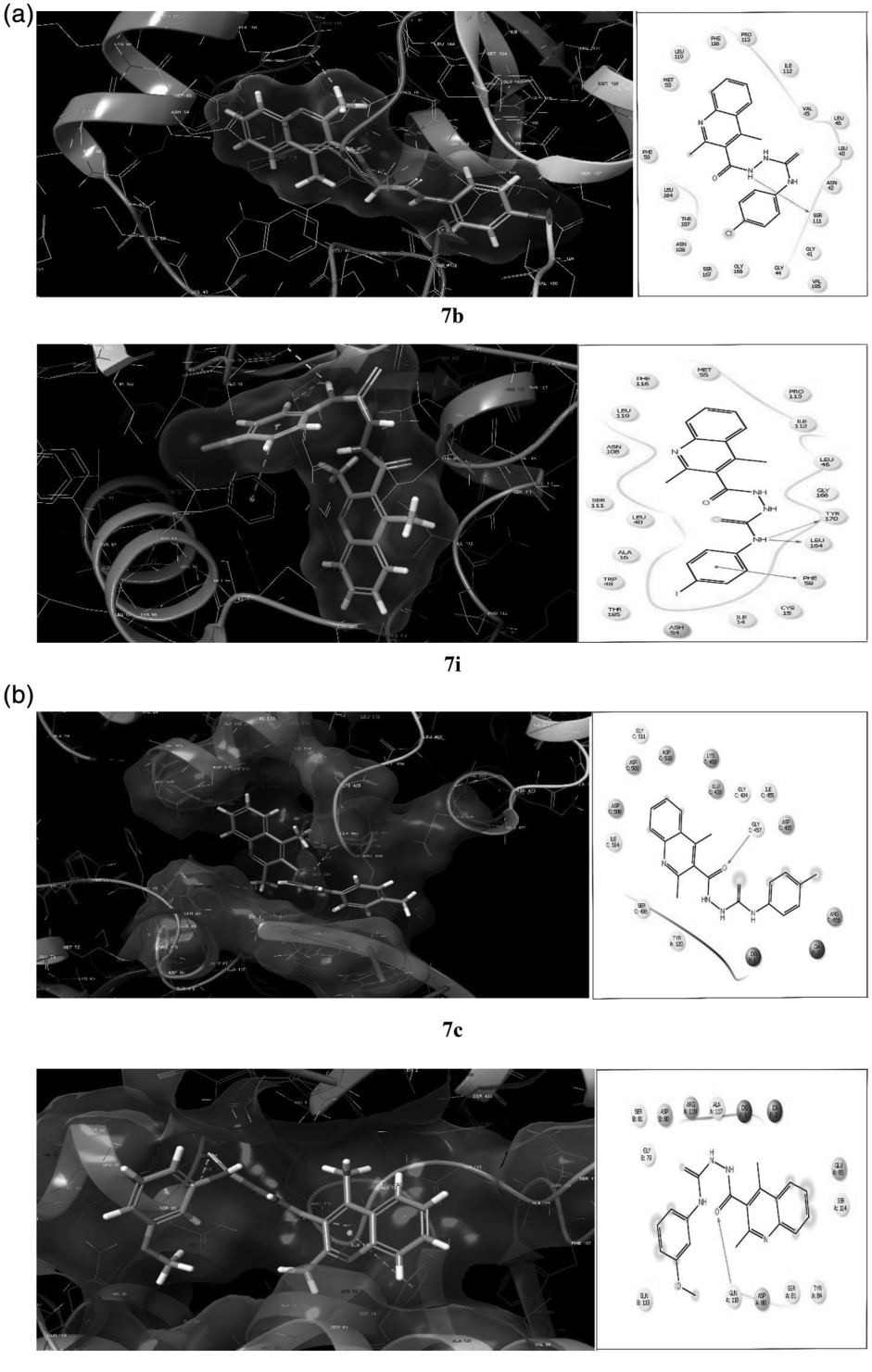

FIGURE 3 A, Binding mode of **7b** and **7i** into active site of *3JSU*. B, Binding mode of **7c** and **7l** into active site of *4DP3*

results with respect to standard drugs. Compounds **7b** and **7n** show moderate activity against the first-line drugs isoniazid and rifampicin. The results are summarized in Table 2.

5.2 | Computational study

5.2.1 | Docking study

Molecular docking is a structure-based drug design that became an important part of drug discovery telling the knowledge of binding sites, binding energy, affinities, and thermodynamic properties of protein-ligand complexes. Therefore, with the aim of promising active drug molecules from the current biological activity of all titled compounds, we investigated the molecular basis of their interaction, and a molecular docking study against *PFDHFR-TS* on *3JSU*, *4DP3*, and *1J3K* were carried out using Glide-based Ligand Docking with Energetics on Glide program of Schrodinger molecular modeling suite. From the docking study, it is clear that four molecules (**7b**, **7e**, **7i**, and **7q**) of substituted derivatives of quinoline compounds could closely fit into the active site of *3JSU*, one molecule (**7g**) of title compound could closely fit into the active site of *4DP3*, and three molecules (**7c**, **7l**, and **7p**) of substituted derivatives of quinoline compounds could closely fit into the active site of *4DP3* and coordinate very similar to the native ligand in the crystal structure; two molecules (**7b** and **7l**) were found to be closely bound into the active site of *1J3K*. A complex of *PFDHFR-TS* was stabilized by the formation of significant closely bound with bonding and nonbonding, various interaction through active site of amino acid and other interaction also observe with reference ligand to the standard inhibitors.

The binding energy of all molecules was found in the negative, which signifies the energy required for the formation of interaction with the active site of complex. The lower the value of binding energy, the stronger is the affinity towards the active site. As per the docking analysis, the docking energy of PDB: *3JSU* was found between −5.38 and −9.59 kcal/mol; for PDB: *4DP3*, between −4.60 and −7.23 kcal/mol; and for PDB: *1J3K*, between −1.98 and −3.54 kcal/mol. In these cases, compounds **7b** and **7i**; compounds **7c** and **7l**; and compounds **7b** and **7l** have shown the least binding energy with the protein PDB: *3JSU*, *4DP3*, and *1J3K*, respectively. From Table 3, we

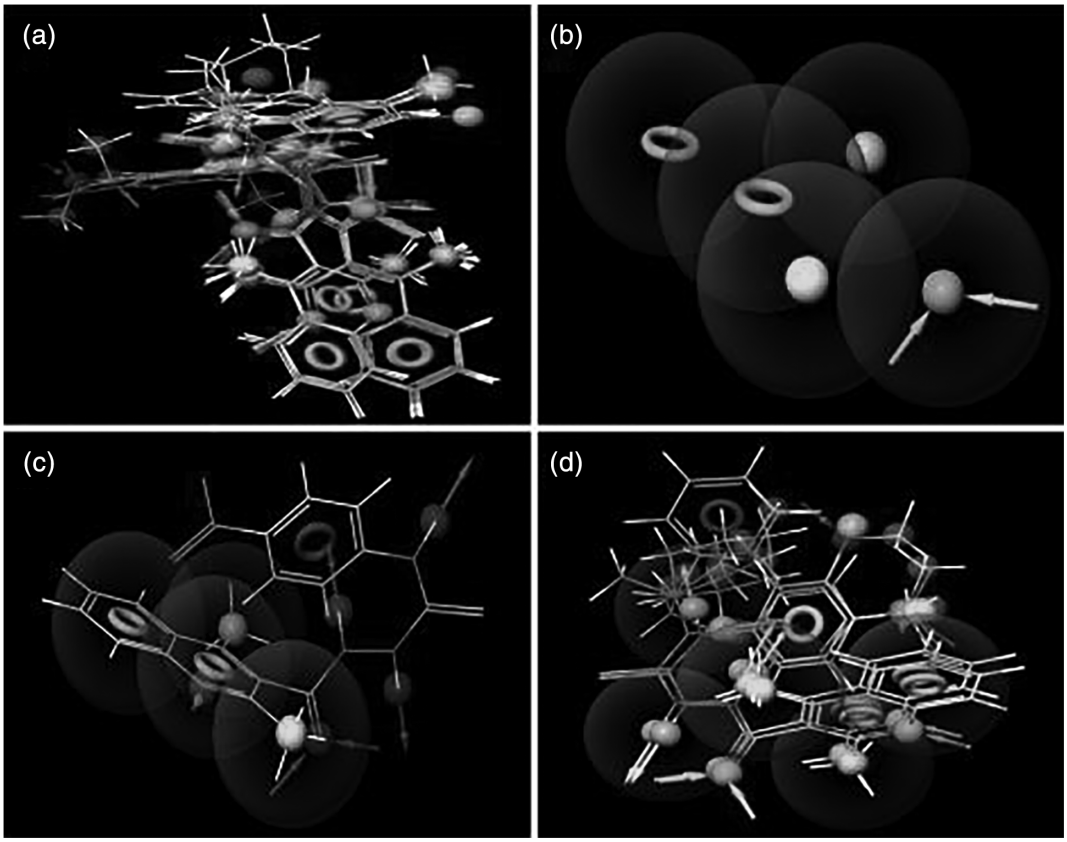

FIGURE 4 (a), Superimposition of pharmacophore generation. (b), The pharmacophore model hypothesis of DHHRR. (c), Pharmacophore model of DHHRR aligned with the highest active compound in the dataset. (d), Superimposition of various hypothesis

have found potent molecules with respect to biological activity. which lead to the further study of such compounds **7b** (−8.32) and **7i** (−8.22) in PDB: *3JSU*, compounds **7c** (−7.23) and **7l** (−5.82) in PDB: *4DP3*, and compounds **7b** (−4.323) and **7l** (−3.039) in PDB: *1J3K*. Compounds **7b** and **7i** are found to be stabilized with active site through Van der Waals interactions with LEU 164, PHE 116, PRO113, VAN 45, LEU 46, ASN 42, and SER 111 residue and interaction with ASN 108, SER 111, LEU 45, TYR 170, LEU 164, and ASH 54 residue through the nucleus (Figure 3a). Compounds **7c** and **7l** are bound to be stabilized with active site through Van der Waals interaction with GLY 457, ASP 435, GLY 434, LYS 458, and ASP 510 and ASP 80, ARG 119, ALA 117, GLN 118, and ASP 80 through the nucleus (Figure 3b). Furthermore, each of the molecules was interacted in hydrogen bond with the active site of residues. The compounds **7b** exhibited hydrogen bonding between —NH— of the thiosemicarbazide linkage and residue SER 111 with the bond length 2.0 A^o and **7i** exhibited hydrogen bonding between —NH— of the thiosemicarbazide linkage and residue TYR 170, LEU 164 with the bond length 2.3 A^o, 2.6 A^o. A very important π- π interaction also found between substituted aromatic ring (compound **7i**) and PHE 58 residue in the active site. The compounds **7c** and **7l** exhibited hydrogen bonding between the oxygen atom of linkage and hydrogen atom of amino acid GLY 457 and GLN 118, respectively, with the bound length with 2.3 A^o, 2.1 A^o. And π- π interaction was found between quinoline ring (compound **7l**) and GLU 122 residue in the active site. Electrostatics and other interaction of compounds are described in

TABLE 4 Predicted ADME-Tox parameter for the title compounds **7a**-**7s**

Product Code	Percent Human Oral Absorption	QPPCaco	QPlogBB	QplogKhsa	QPlogHERG	QPlogS	PSA
7a	85.871	163.789	−1.557	0.437	−6.469	−6.092	122.152
7b	100	1369.894	−0.273	0.581	−6.47	−6.636	77.235
7c	100	1369.328	−0.454	0.621	−6.465	−6.46	77.232
7d	100	1264.592	−0.514	0.275	−5.499	−5.038	77.876
7e	100	1369.234	−0.144	0.683	−6.378	−7.238	77.238
7f	100	1369.234	−0.144	0.683	−6.378	−7.238	77.238
7g	100	1404.59	−0.438	0.447	−5.615	−5.831	75.405
7h	100	1476.362	−0.481	0.59	−6.831	−6.426	77.065
7i	100	1368.702	−0.512	0.488	−6.444	−6.147	85.525
7j	100	1370.393	−0.253	0.629	−6.53	−6.876	77.235
7k	100	1369.134	−0.117	0.692	−6.372	−7.361	77.242
7l	100	1854.969	−0.347	0.483	−6.36	−5.957	82.753
7m	100	1367.189	−0.513	0.486	−6.41	−6.07	85.478
7n	100	1369.031	−0.016	0.785	−6.282	−7.832	77.245
7o	100	1839.495	0.032	0.679	−6.25	−7.122	76.159
7p	100	1692.196	−0.127	0.543	−6.219	−6.395	76.665
7q	100	1259.928	−0.426	0.172	−5.3	−4.864	78.181
7r	100	1370.052	−0.428	0.471	−6.56	−5.91	77.233
7s	100	1379.78	−0.449	0.592	−5.638	−6.222	77.084
7a	86.134	516.801	−0.606	−0.136	−4.632	−3.701	92.489
Quin*	100	821.804	0.211	0.243	−5.45	−3.3	42.892
CQ*	100	1436.68	0.397	0.597	−6.415	−4.641	26.062
INH*	66.893	277.474	−0.842	−0.752	−3.592	−0.052	81.354
Cipro*	52.666	22.644	−0.389	−0.059	−2.953	−3.772	93.3
NRFX*	47.412	20.376	−0.5	−0.171	−2.991	−3.446	93.483

Note: %, human oral absorption in GI (±20%). QPPCaco, Apparent Caco-2 permeability (nm/s) (500 great); QPlogHERG, HERG K + channel blockage (concern below −5); QPlogP, octanol/water (−2.0, − 6.5); QPlogS, Predicted aqueous solubility, (−6.5, − 0.5).

Figure 3. Such hydrogen bonding and π- π stacking interactions are very crucial as they serve as an "anchor" guiding the 3D orientation of the ligand in its active site and also facilitate the steric and electrostatic interactions adding to the stability of the enzyme-inhibitor complex. Figure 3a,b showed the binding mode of compounds **7b**, **7i**, and compounds **7c**, **7l**, respectively; other binding mode of compounds are shown in Supporting Information.

5.2.2 | Pharmacophore model

A feature of pharmacophore model was used to identify the important interaction with proteins. On the basis of activity, molecules were divided into three groups: low, moderate, and high activity. High active groups were selected as representative of a common pharmacophore generation. Default interaction features such as acceptor (A), donor (D), hydrophobic (H), positive ionisable (P), negative ionisable (N), and ring aromatic (R) were used for generating favorable pharmacophore models. In addition, three common features, DHHRR, AHHRR, and AHHPR, were selected for the pharmacophore generation (Figure 4). In summary, the common five-feature model DHHRR was selected for the best pharmacophore generation. For the DHHRR model, a total of 13 actives in the dataset and 12 actives were recovered in the dataset to 93% to active recovered. Other model AHHRR and AHHPR show similar results with 60% and 79%

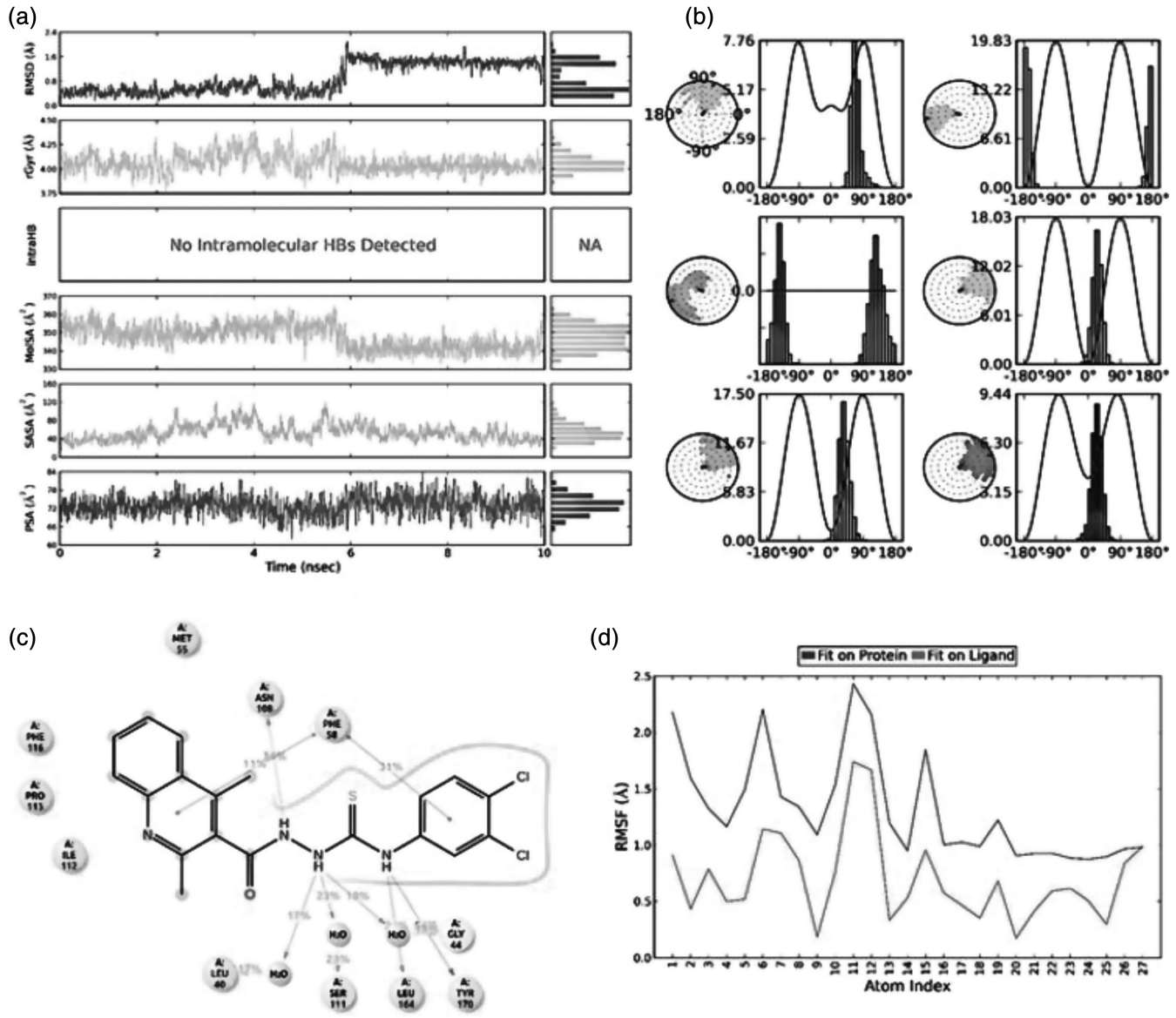

FIGURE 5 Simulation interaction with ligand (**7e**). (a), Ligand interaction properties. (b), Ligand torsions. (c), Ligand protein contacts in 2D. (d), Ligand protein RMSF. (e), Protein ligand interaction. (f), Protein ligand RMSD. (g), Protein RMSF

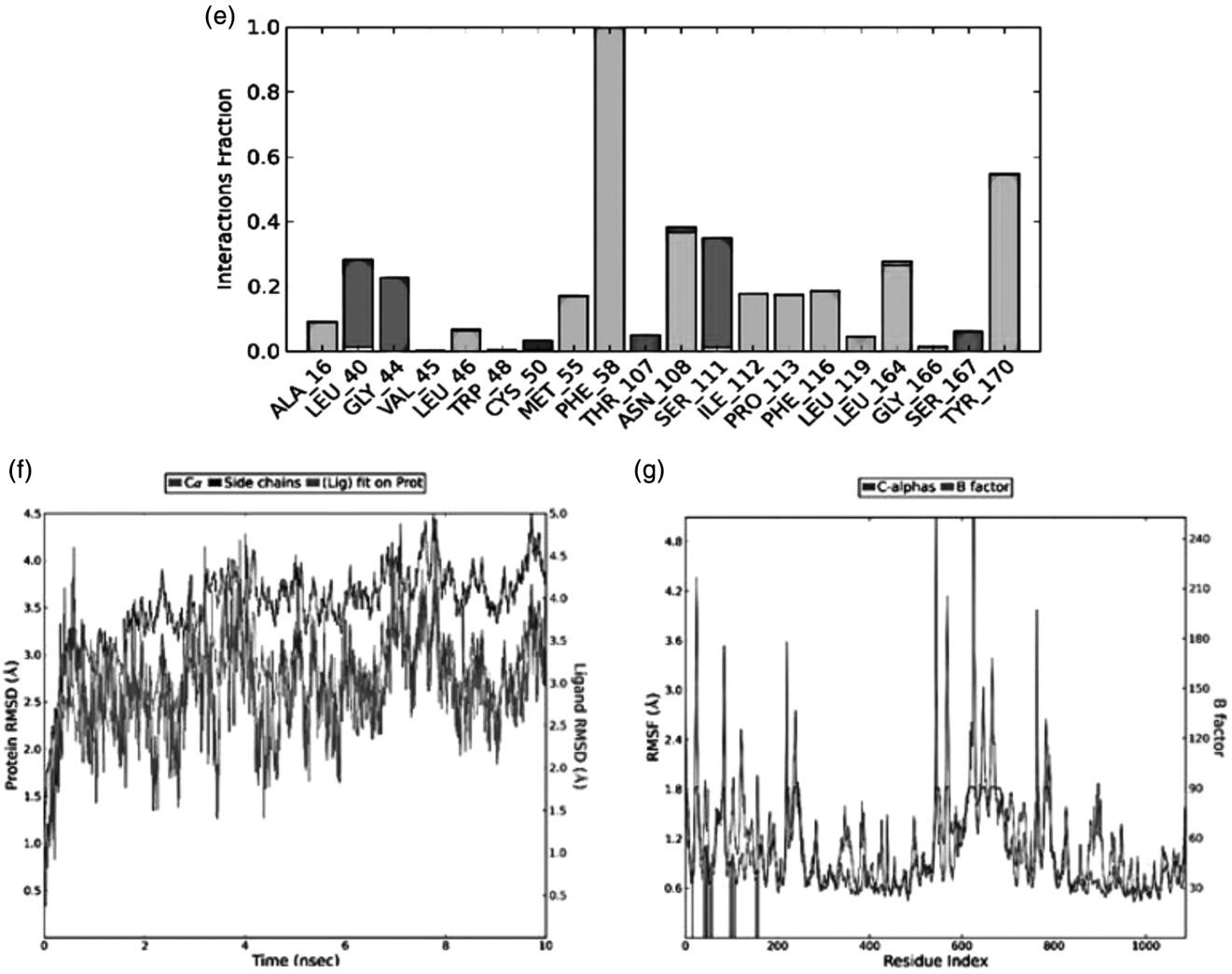

FIGURE 5 (Continued)

active recoverability performance. Here, the survival score of DHHRR, AHHRR, and AHHPR are 6.308, 6.097, and 6.023, respectively. Moreover, AHRR shows a poor performance with 1.361 survival score. As per these results, we continue our research with the pharmacophore modeling with our knowledge.

5.2.3 | ADME-Tox study

The title molecules (**7a**-**7s**) were evaluated for their in silico pharmacokinetics properties leading to drug-likeness using Qikpro (Schrödinger, LLC, New York, NY, 2018). The Jorgensen method was utilized by the program Qikpro for the pharmacokinetics properties and descriptors.[37] It can give a very good idea about which compounds deserved further attention for evaluation.[38] The compute ADME-Tox parameters along with their acceptable limits are as indicated in Table 4. Various descriptors of Qikpro such as Polar surface area (PSA) (70-200 Å) as the oral bioavailability, percent human oral absorption (80% to 25%), Caco-2 cell permeability (QPPCaco) as model for gut-blood barrier (25 to 500), QPlogkhsa as human serum albumin binding (−1.5 to 1.5), QPlogBB as blood/brain partition coefficient (−3.0 to −1.5), QPlogS as aqueous solubility parameter (−6.5 to 5), and QPlogHERG (below −5) are described in Table 4. Analog **7f**, **7j**, and **7o** found to be in good bioavaibility with described range.

5.2.4 | Molecular dynamics

In these studies, a behavior and simulation of best docked compound **7e** with PDB: *3JSU* were investigated by using molecular dynamics simulation. Compound **7e** was formed open catalytic activity with *A: Leucine 40*, *A: Serine 111*, *A: Leucine 164*, *A: Tyrosine 170*, *A: Glycine 44*,

A: Asparagine 108. The various energy, ligand properties, hydrogen bond, and Van der Waals force have been notified with various levels in the study. According to the interaction and forces, compound **7e** fluctuated at some levels yielding an RMSD value of 2.2 A°. Figure 5 showed that protein and ligand were similarly fluctuated in the system with a range of 0.3 to 2.4 A°. Figure 5 showed protein-ligand π-π interaction with *Phenylalanine 58* and *ALA 16*, *VAL 45*, *LEU 46*, *TRP 48*, *CYS 50*, *MET 55*, *THR 107*, *ASN 108*, *ILE 112*, *PRO 113*, *PHE 116*, *LEU 119*, *LEU 164*, *SER 167* amino acids formed various interactions in the simulation. The analysis results of the simulation are shown in Figure 5.

6 | CONCLUSIONS

In conclusion, we have synthesized a series of quinoline hybrid thiosemicarbazide derivatives under microwave irradiation. Synthesized compounds were successfully applied against the biological studies. Compounds **7a**, **7g**, and **7k** exhibited potent activity against *P. aeruginosa*, and compounds **7a**, **7f**, **7h**, and **7r** showed excellent activity against *E. coli*. We noticed that compounds having substitution at 4-position ring exhibited high potency against *P. falciparum*; as a result, compounds **7a**, **7b**, **7c**, **7e**, and **7o** have very good potency as compared with standard drug quinine. Also, compounds **7f**, **7l**, **7p**, **7q**, and **7s** also exhibited good activity against *P. falciparum* strain. Furthermore, the docking study was performed on selected three proteins *3JSU*, *4DP3*, and *1J3K*. Compounds **7b** (−8.32) and **7i** (−8.22) were selected in *3JSU*, compounds **7c** (−7.23) and **7l** (−5.82) were selected in *4DP3* for the best binding possess, and compounds **7b** (−4.323) and **7l** (−3.039) were selected in *1J3K* for the best binding possess. The docking study suggested that the selected molecules were perfect, fitting into the protein cavity with excellent G-score. Moreover, the interaction simulation of the selected compound **7e** with protein (PDB: *3JSU*) were studied by the molecular dynamics study on Schrodinger's software. Pharmacophore study and ADME-Tox were carried out for the drug-likeness properties. This study proved that our molecules could be act as hit molecules in the future.

ACKNOWLEDGMENTS

The authors are thankful to the Department of Chemistry, Gujarat University, Ahmedabad, Gujarat, India for providing the necessary facilities. UGC-Info net and INFLIBNET Gujarat University are acknowledged for providing the e-resource facilities, NFDD Centre for proton NMR and Synzeal laboratory for ESI-MS spectroscopy. The authors are thankful to GUJCOST, Gandhinagar, Gujarat, India for financial support (Project: MRP No. GUJCOST/MRP/2017-18/2323).

CONFLICT OF INTEREST

The authors declare no potential conflict of interest.

ORCID

Hitesh D. Patel https://orcid.org/0000-0002-0664-8874

REFERENCES

[1] S. Eswaran, A. V. Adhikari, N. S. Shetty, *Eur J Med Chem* **2009**, *44*, 4637–47.
[2] C. de la Guardia, S. David, D. Hang, Q. Mario, L. Oleg, L. Ricardo, *Molecules* **2018**, *23*, 672.
[3] A. Kedjadja, A. Bouraiou, R. Merdes, *Int J Org Chem* **2018**, *8*, 105–14.
[4] K. D. Upadhyay, M. D. Narsinh, C. K. Rupesh, S. C. Ravi, K. S. Anamik, *ACS Med Chem Lett* **2018**, *9*, 283–8.
[5] P. Nasveld, S. Kitchener, *Trans R Soc Trop Med Hyg* **2005**, *99*, 2–5.
[6] J. T. Smith, *Eur J Clin Microbiol Infect Dis* **1984**, *1*, 347.
[7] R. Musiol, J. Jampilek, V. Buchta, L. Silva, H. Niedbala, B. Podeszwa, A. Palka, K. Majerz-Maniecka, B. Oleksyn, J. Polanski, *Bioorg Med Chem* **2006**, *15*, 3592.
[8] A. Lilienkampf, J. Mao, B. Wan, Y. Wang, S. G. Franzblau, A. P. Kozikowski, *J Med Chem* **2009**, *52*, 2109–18.
[9] N. C. Warshakoon, J. Sheville, R. T. Bhatt, W. Ji, J. L. Mendez-Andino, K. M. Meyers, N. Kim, J. A. Wos, C. Mitchell, J. L. Paris, B. B. Pinney, *Bioorg Med Chem Lett* **2006**, *16*, 5207–11.
[10] B. Kalluraya, S. Sreenivasa, *Il Farmaco* **1998**, *30*, 399.
[11] S. Mukherjee, M. Pal, *Drug Discov Today* **2013**, *18*, 389–98.
[12] A. Mahamoud, J. Chevalier, A. Davin-Regli, J. Barbe, *Curr Drug Targ* **2006**, *7*, 843–7.
[13] N. Murugananthan, R. Sivakumar, N. Anbalagan, V. Gunasekaran, J. T. Leonard, *Biol Pharm Bull* **2004**, *27*, 1683–7.
[14] M. P. Maguire, K. R. Sheets, K. McVety, A. P. Spada, A. Zilberstein, *J Med Chem* **1994**, *37*, 2129–37.
[15] N. Ahmed, K. G. Brahmbhatt, S. Sabde, D. Mitra, I. P. Singh, K. K. Bhutani, *Bioorg Med Chem* **2010**, *18*, 2872–9.
[16] L. Strekowski, J. L. Mokrosz, V. A. Honkan, A. Czarny, M. T. Cegla, S. E. Patterson, R. L. Wydra, R. F. Schinazi, *J Med Chem* **1991**, *34*, 1739–46.
[17] S. S. Sonar, S. A. Sadaphal, V. B. Labade, B. B. Shingate, M. S. Shingare, *Phosphorus, Sulfur Silicon Relat Elem* **2009**, *185*, 65.
[18] K. Nakatani, S. Sando, I. Saito, *Bioorg Med Chem* **2001**, *9*, 2381–5.
[19] A. Y. Usyatinsky, Y. L. Khmelnitsky, *Tetrahedron Lett* **2000**, *41*, 5031–4.
[20] R. H. Manske, M. Kulka, *Organic Reactions* **2004**, *7*, 59.
[21] M. Matsugi, F. Tabusa, J. I. Minamikawa, *Tetrahedron Lett* **2000**, *41*, 8523–5.
[22] N. P. Buu-Hoi, R. Royer, N. D. Xuong, P. Jacquignon, *J Org Chem* **1953**, *18*, 1209–24.
[23] J. Marco-Contelles, E. Perez-Mayoral, A. Samadi, M. D. Carreiras, E. Soriano, *Chem Rev* **2009**, *109*, 2652–71.
[24] V. V. Kouznetsov, L. Y. Mendz, C. M. M. Gomez, *Curr Org Chem* **2005**, *9*, 141–61.

[25] J. Wu, H. G. Xia, K. Gao, *Org Biomol Chem* **2006**, *4*, 126–9.
[26] S. J. Song, S. J. Cho, D. K. Park, T. W. Kwan, S. A. Jenekhe, *Tetrahedron Lett* **2003**, *44*, 255–7.
[27] M. A. Zolfigol, P. Salehi, A. Ghaderi, M. Shiri, *Catal Commun* **2007**, *8*, 1214–8.
[28] P. Hawkey, D. Lewis, *New York*, Oxford University Press, NY **2003**.
[29] K. H. Rieckmann, G. H. Campbell, L. J. Sax, J. E. Ema, *The Lancet* **1978**, *311*, 22–3.
[30] L. A. Collins, S. G. Franzblau, *Antimicrob Agents Chemother* **1997**, *41*, 1004–9.
[31] T. A. Halgren, R. B. Murphy, R. A. Friesner, H. S. Beard, L. L. Frye, W. T. Pollard, J. L. Banks, *J Med Chem* **2004**, *47*, 1750–9.
[32] R. A. Friesner, J. L. Banks, R. B. Murphy, T. A. Halgren, J. J. Klicic, D. T. Mainz, M. P. Repasky, E. H. Knoll, M. Shelley, J. K. Perry, *J Med Chem* **2004**, *47*, 1739–49.
[33] R. A. Friesner, R. B. Murphy, M. P. Repasky, L. L. Frye, J. R. Greenwood, T. A. Halgren, P. C. Sanschagrin, D. T. Mainz, *J Med Chem* **2006**, *49*, 6177–96.
[34] D. G. Daraji, K. D. Patel, H. D. Patel, D. P. Rajani, *J Heterocycl Chem* **2019**, *56*, 539–51.
[35] D. B. Patel, K. D. Patel, N. P. Prajapati, K. R. Patel, D. P. Rajani, S. D. Rajani, N. S. Shah, D. D. Zala, H. D. Patel, *J Heterocycl Chem* **2019**, *58*, 00.
[36] E. M. Duffy, W. L. Jorgensen, *J Am Chem Soc* **2000**, *122*, 2878–88.
[37] D. B. Patel, R. H. Vekariya, K. D. Patel, M. S. Vasava, D. P. Rajan, S. D. Rajani, H. D. Patel, *J Heterocycl Chem* **2018**, *55*, 632–44.
[38] QikProp, Technical Information, https://www.schrodinger.com/qikprop

SUPPORTING INFORMATION

Additional supporting information may be found online in the Supporting Information section at the end of this article.

How to cite this article: Patel DB, Darji DG, Patel KR, Rajani DP, Rajani SD, Patel HD. Synthesis of novel quinoline-thiosemicarbazide hybrids and evaluation of their biological activities, molecular docking, molecular dynamics, pharmacophore model studies, and ADME-Tox properties. *J Heterocyclic Chem*. 2020;1–18. https://doi.org/10.1002/jhet.3855